An optical fiber-based gating device for prospective mouse cardiac MRI.

Raphaël Sablong, Adrian Rengle, Anoop Ramgolam, Hervé Saint-Jalmes, Olivier Beuf

An optical fiber-based gating device for prospective mouse cardiac MRI

R. Sablong, A. Rengle, A. Ramgolam, H. Saint-Jalmes and O. Beuf

***Abstract*—Prospective synchronization of MRI acquisitions on living organisms involves the monitoring of respiratory and heart motions. The electrocardiogram (ECG) signal is conventionally used to measure the cardiac cycle. However, in some circumstances, obtaining an uncorrupted ECG signal recorded on small animals with RF pulses and gradient switching is challenging. To monitor respiratory motion, an air cushion associated with a pressure sensor is commonly used but the system suffers from bulkiness. For many applications, the physiological gating information can also be derived from an MR navigated-signal. However, a compact device that can simultaneously provide respiratory and cardiac information, for both prospective gating and physiological monitoring, is desirable. This is particularly valid since small volume coils or dedicated cardiac RF coil arrays placed directly against the chest wall are required to maximize measurement sensitivity. An optic-based device designed to synchronize MRI acquisitions on small animal's respiratory and heart motion was developed using a transmit-receive pair of optical fibers. The suitability of the developed device was assessed on mice (n=10) and was based on two sets of experiments with dual cardiac and respiratory synchronization. Images acquired with prospective triggering using the optical-based signal, ECG and the pressure sensor during the same experiment were compared between themselves in the first set. The second set compared prospective technique using optical-based device and ECG to a retrospective technique. The optical signal which was correlated to both respiratory and heart motion was totally unaffected by radiofrequency pulses or currents induced by the magnetic field gradients used for imaging. Mice heart MR images depict low visible motion artifacts with all sensors or techniques used. No significant SNR differences were found between each series of image. Full fiber optic based signal derived from heart and respiratory motion was suitable for prospective triggering of heart MR imaging. The fiber optic device performed similarly to the ECG and air pressure sensors, while providing an advantage for imaging with dedicated cardiac array coils by reducing bulk. It can be an attractive alternative for small animal MRI in difficult environments such as limited space and strong gradient switching.**

***Index Terms*—Cardio-respiratory triggering, optical sensor fibers, prospective, retrospective triggering, mouse heart MRI.**

I. Introduction

There has been a rising interest for small animal Magnetic Resonance Imaging and Spectrometry (MRI-MRS) since many years. The growing number of animal models and recent advances in dedicated NMR instruments are contributing to the current abundance of studies on the vascular, cardiac and abdominal systems as well as on the brain, typically in mice and rats. In most cases, suitable images and spectra are achieved through the implementation of triggering methods. Indeed, movements of the rib cage (ventilation) and the heart (heartbeat) generate artifacts that can significantly impair the quality of acquired images and spectra, especially when high spatial resolution is required [1]. These movements are not only due to the heart and lungs, but also have a systemic character. Artifacts appear mainly as localized blurring or ghosting propagating along the phase encoding direction in imaging and as line broadening in spectroscopy. The extension and intensity of these movement artifacts depend on various parameters such as physiological conditions (anesthesia, species...), mechanical properties (studied organ, volume available...) and acquisition constraints (spatial or temporal resolution, sequence used…). Several strategies were implemented to mitigate the effect of these movements.

Different methods using prospective cardio-respiratory synchronizations are widely used for acquisitions of this kind. The NMR signal is acquired only at appropriate timings concurring to a real-time signal obtained from the measurement of the animal's movements due to breathing and heartbeat cycle. The former is composed of a fast inspiration phase and a slow end expiration phase. One of the ways of differentiating these two phases during which the acquisition can take place, is to use a pneumatic system where a balloon is placed on the animal's abdomen and allows respiratory movement monitoring through pressure fluctuations. Another common technique consists of using an Electrocardiogram (ECG). The electro-physiological signal is an accurate signature of the heart beat with successive waves defining the different heart phases (diastolic, systolic); this either allows an acquisition to be performed at a specific phase of the heart beat or to acquire several frames of the heart cycle followed by CINE movies reconstruction. However, Radio frequency (RF) field and fast gradient switching can induce currents along the ECG leads that can potentially disturb the ECG signal and additionally induce localized heating of the region sporting the electrodes. Non-metallic materials like carbon wires have been proposed almost 25 years ago [2] and is still an active research area [3]. While carbon leads are reducing heating, the use of carbon wires alone is not sufficient to solve induced ECG artifacts in worst cases. Such

approach has to be combined with an electro-optical conversion module to be really efficient. A second electro-optical conversion module placed at a convenient distance from the magnet converts the optical signal into an electrical signal that can be processed by the triggering device [4]. An ECG-based device often spares the use of an additional breathing sensor by using the modulation of the ECG by a low frequency wave associated with ventilation. Specific signal processing allows discriminating the two physiological signal sources and thus to perform a dual cardio-respiratory synchronization.

Several studies [5, 6] reported challenging cardiac synchronization using ECG especially for cardiac microscopy when short repetition time and high gradient-slew rate are used. Quite a few studies have sorted several alternatives and tested them successfully. Respiratory-gated and cardiac-triggered spin-echo images of the rat abdomen and mouse heart were performed with an inductive pickup coil placed on the animal's chest instead of using standard ECG leads [7] but the method is not optimal for use with RF surface coils or arrays for cardiac imaging. Other straightforward optical detection systems, based on the interruption of an infrared optical beam, have previously been proposed for respiratory gating only [8]. Detection without contact, based on the infrared reflectometry principle has previously been characterized by Lemieux [9]. Different authors have used a dedicated bed to facilitate the non-invasive placement of an optical probe coupled to optical fibers for mice liver examination at 4.7T [10] and 7T [11]. The ease of use and low cost of the fiber-optic detector was further demonstrated on mouse liver by enabling respiratory-synchronized 1H MR Spectroscopy acquisition [12].

Studies based on optical detection to measure the cardiac motion are scarce. Only a handful of studies pertaining to few invasive or minimally invasive methods unaffected by RF fields and gradient switching can be found in the literature. An invasive miniature optical probe inserted into an artery showed an optical signal resulting from a fluctuating light reflection caused by the pulsatile blood flow [13]. A second study described an optical stethoscope where an optical fiber was carefully introduced into the animal's esophagus and the fiber tip then placed close to the mouse's heart. A signal correlated to the cardiac cycle was then measured via this setup [14]. However, positioning the probe at the exact location requires expertise and hence limits the widespread diffusion of such minimally invasive technique. More recently, the reliability of a cardio-acoustic triggering device for human cardiac CINE imaging at 7T [15] as well as the feasibility to use MagnetoHydroDynamic (MHD) effects for synchronization of MR acquisitions with the cardiac cycle [16] were demonstrated.

On another hand, retrospective techniques based on navigated-signal do not require any sensors. However they are not compatible with all acquisitions. Rectilinear self-navigated motion detection techniques were first proposed for human cardiac imaging [17, 18] and extended to abdominal imaging [19]. This technique eliminates the need for an ECG or respiratory signal by recording a motion synchronization signal directly from non-triggered navigator data. A navigated signal, acquired without phase or readout gradients, is used to achieve retrospective gating ahead of image reconstruction.

Abiding to the context, this study aims at comparing the prospective triggering techniques with a retrospective technique. Three types of sensors capable of monitoring the heart beat and the breathing cycle were used: (a) reflected light modulation using an original device with optical fibers, (b) ECG, (c) pressure sensor via air cushion. Images were obtained from a short axis-orientation mouse cardiac CINE FLASH sequence and compared between themselves. The goal of this study was to demonstrate that optical fiber is a suitable alternative for dual cardio-respiratory gating without the limitations of ECG or respiratory pillow.

II. Experimental

A. Optical gating device

The optical probe consists of a bundle of two silica multimode optical fiber of 200 μm core diameter (one for light transmission and one for light detection). Distal parts were stripped (2 cm long), cleaved and polished to maximize light detection and the two fibers were afterwards glued together. Each fiber was optically insulated with thin heat shrink cover to minimize the ambient light noise. Once assembled, the optical probe is a thin and soft cylindrical line of less than 2mm diameter with a junction at about 5 cm apart from the tip enlarging punctually the diameter to 3 mm. The proximal part of the transmit fiber was connected to a 820 nm wavelength 100 μW transmit power HFBR-1405 light emitting diode (LED) whereas the detection fiber was connected to a HFBR-2405 light-voltage amplified photodiode receiver (Agilent Technologies, CA, USA). The transmit fiber was used to illuminate the moving surface and the receiver fiber captured a fraction of the backscattered light. This quantity of light is modulated by the cardio-respiratory movements of the animal's chest. After conversion of the modulated light into an electrical signal, the latter was passed through a custom-built signal-processing circuit for further amplification and filtering. This circuit consisted of two active wide band pass filter placed before and after an amplifier with adjustable gain. Each active wide band pass circuit was composed of two active second order high pass filters and two active second order low pass filters. The corner frequencies were 0.2 Hz and 30 Hz respectively. The repetition rate of the mice's heart beat is typically about 5 to 10 Hz while

that of the ventilation movement varies between 0.5 to 1 or 2 Hz. These physiological frequencies are included in the filter passband. Any continuous component of the signal is filtered out and the upper cutt-off frequency, together with a fourth order filter profile, enables to greatly reject 50 Hz residues due to any parasitic galvanic coupling to power supply. The filter design was based on a Sallen-Key topology. The amplifier stage with adjustable gain was conceived using an operational amplifier in an inverting configuration with a 100/1,000/10,000 scale for an adjustable gain. A fixed gain of 10,000 was selected. With a narrow bandwidth (30 Hz) and the use of low noise operational amplifiers for active filtering and amplification, high signal-to-noise detection can be performed. The processed output signal was then connected to a commercial Trigger Unit HR V2.0 (Rapid Biomedical, Würzburg, Germany) for gating purpose (Fig. 1).

B. Optical gating device characterization

The characteristics of the optical-based device were measured using a calibrated light source. A light intensity modulated laser (670 nm, 1 mW average power, Laser Components GMBH, Germany) was used to illuminate the fiber tip all while the beam being attenuated by a white screen to avoid detector saturation. The device transfer function was assessed frequency-wise. The laser intensity modulation frequency was controlled by means of a standard 33220A low frequency generator in sweep mode (Agilent technologies, CA, USA). The input and output signals were both recorded using a data acquisition board with Labview® Software Interface (National Instruments, USA). Thus to check whether the measured Bode diagram fits the expected specifications, the harmonic response of the device is accurately determined in terms of amplitude and phase. Besides, the transient response to a typical input signal was also investigated: the impact of the frequential characteristics of the filter on the waveform of the signal corresponding to mouse monitoring is better illustrated in the time domain. Indeed the waveform of the measured signal is determined by both the optical and mechanical processes (which characterize light propagation within a complex medium, in our case the tissue) and the bandpass of the filter. The latter being quite narrow (30 Hz), the output signal is inevitably distorted and thus denies access to the "real" input signal. Therefore an approximated input signal in the form of an ECG-like waveform mirroring the heart activity was used to illustrate the distortions induced by the filter. This signal (since the input signal is unknown) was generated using the 33220A generator set in arbitrary waveform mode to drive the modulated laser intensity. An ECG-like signal was generated from a specific 512 data points file (.csv format) coded in Matlab (http://www.mathworks.com/matlabcentral/fileexchange/10858-ecg-simulation-using-matlab) using the template described in reference [20]. The main waveform features were the P,Q,R,S,T waves from which the amplitude, shape and phase were set to be comparable to the typical physiological parameters of mouse heart beats. The repetition rate of this temporal pattern was set to be 6.6 Hz.

The optical device response was compared to the driving signal. Finally an optical power meter enabled to measure the minimum and maximum intensity in milliwatts of the modulated light source.

C. Experimental in vivo setup

Triggering efficiency was assessed through image quality acquired on ten OF1 mice (6 weeks old with 26±2 g average weight). The first series was dedicated to prospective triggering with successive acquisitions performed on each mouse using the optical, ECG and pressure signals respectively. The optical fiber pair was first fixed on the thorax using soft medical adhesive tape. For ECG, the front paws were wrapped in copper foil and the peripheral ECG signal was derived via silver wire. To minimize both corrupted signal and heating due to gradient switching [21], the loop formed by the paws and the cable ends was kept as small as possible by twisting both wires. The screened 2-wire ECG cable was then guided straight in the z-direction through the magnet close to the symmetry axis. Special care was taken in these experimental conditions not to be in a worst case scenario and avoid ECG signal failure with the commercial triggering unit available at the laboratory. Finally, the air cushion was placed above and taped on the fiber tips (Fig. 2). The air cushion was a 20 mm diameter and 3 mm thick soft disk connected by a 2 mm outer diameter catheter to a deported pressure sensor. Approximately the same delays, low and high cutoff frequencies for filtering were applied on the ECG trigger unit. Typical signals from these sensors have been recorded to show that the different devices provide comparable real-time information about cardiac and breathe movements of a given animal. Two days later, a second series of acquisitions on the same mice was performed with prospective triggering using optical and ECG sensors and a retrospective triggering sequence. The experimental protocol was approved by the Animal Ethics Committee of our institution and ethical guidelines for experimental investigations with animals were strictly followed. A dedicated anesthesia system (TEM, Lormont, France) using isoflurane gas was used to perform the anesthesia. Induction was realized with 4% gas mixed with air administrated at 1°L/min flow. The animals were placed in a supine position on a dedicated plastic bed with circulating warm water for body temperature regulation while anesthesia was maintained during MRI examination with 2% isoflurane mixed with air at 0.6 to 1 L/min flow. A capillary filled with a 1.25 g/L $NiSO_4$ solution and placed below the mouse was used as an external image reference.

D. Imaging protocol

Experiments were performed on a 4.7T Biospec system (Bruker, Ettlingen, Germany) with a quadrature 32 mm inner diameter birdcage coil (Rapid Biomedical, Würzburg, Germany). Short axis-orientation images of the heart were obtained using a CINE FLASH sequence with the following parameters: 30 x 30 mm^2 field-of-view (FOV), 256x192 matrix, 4 averages; phase anti-aliasing=2; TR/TE=9/2.9 ms; 25° flip angle; 1 mm slice thickness; 50 kHz receive bandwidth. With an average heart rate of 400 bpm, a total of 12 frames per heart cycle was obtained. For the first series, a Black Blood (BB) CINE FLASH sequence was additionally performed with 6 frames and a 120 ms time of inversion (TI), using optics and ECG signals. For each prospectively-gated acquisition series, cardiac and respiratory periods as well as total scan duration were recorded.

For retrospective gating, the IntraGateFLASH method from Bruker was used. The read- and phase-dephase gradients were separated from the slice-refocusing gradient in order to detect a half echo signal without phase encoding. The navigator was then derived from the selectively excited slice. It is worth noting that this technique is restricted to a single slice, since the navigators from neighboring slices cannot be combined. The imaging parameters were TR/TE=10.3/4.2 ms; 1.1 mm slice thickness; 200 repetitions for 6 min 36 sec total scan time. Other acquisition parameters were identical to those used in the FLASH method. CINE image reconstruction was performed with one respiration frame and 12 heart frames to be consistent with prospective parameters.

Finally, the efficiency of the optical gating device was also assessed on mice liver using a dual cardio-respiratory triggering. An axial fat suppressed (FS) multiple Spin-Echo (SE) sequence was used with the following parameters: 30x30 mm^2 FOV; 0.7 mm slice thickness; TR=6000 ms; TE=20, 40 and 60 ms; 256x192 matrix, 24 slices using previously describe acquisition strategy [22, 23].

E. Image analysis

For heart imaging, a region of interest (ROI) corresponding to the left ventricular myocardium wall was drawn manually on every single CINE image using CreaContour (in-house developed software). Mean signal intensity and surface area in the ventricular cavity and in the myocardium wall were calculated. The signal-to-noise ratio (SNR) in the left ventricular myocardium was then assessed by dividing the average signal intensity by the standard deviation (SD) of the image background noise level in an out-subject region free of ghosting artifacts. The contrast-to-noise ratio (CNR) value was computed as the SNR difference measurement between the myocardium wall and the left ventricular cavity which corresponds to the end-diastolic phase with no flow artifacts.

For each series, significant differences between SNR, CNR, scan time and physiological period values measured with the different sensors or techniques were determined using a paired Student's t test (Excel, Microsoft, WA, USA). For liver imaging, the efficiency of the optical-based triggering signal was simply assessed based on a visual analysis.

III. Results

A. Optical device

The complex transfer function of the optical device was measured. Amplitude and phase were plotted against frequency (Fig. 3a). The low and high corner frequencies were higher than 0.3 Hz and higher than 30 Hz respectively. The device response to an ECG-like signal is slightly distorted but retains a similar aspect to the driving signal (Fig. 3b).

However, a typical delay of several milliseconds was systematically observed between each wave of the driving signal (DS) and the corresponding response signal (RS). For instance a time shift of 14 ms was measured between the R-wave of RS and the corresponding component of DS. This induces a delay of about 10% of the cardiac cycle duration between the thorax motion signal and the trigger unit's output when the optical device is used compared to ECG or pressure sensors. Moreover, the shape of the main waves is modified as the output waveform is smoothed by the filter. The measured sensitivity of the device within the bandwidth was typically 25 mV output voltage per nW of input light.

B. Optical-based motion signal

Only a few seconds were necessary to install the optical probe correctly and visualize a signal with both cardiac and respiratory components. The signal is comprised of distinct peaks representing respiratory and heart motions respectively (Fig 4a). The largest peaks are attributed to breathing while the smaller oscillations to heart motion. The electromagnetic perturbations induced by RF pulses and gradient switching did not affect the optical signal. The latter was independent of RF flip angle pulse and sequence used. The signal amplitude was high enough to perform a straightforward adjustment of the gating levels with good differentiation between cardiac and respiratory signal amplitude. Signal amplitude variations due to different experimental conditions such as animal size, animal hair as well as the fiber tip location on the thorax are compensated by the adjustable

amplifier gain. Interfaced with the commercial trigger unit used, the gating levels, delays and acquisition windows were easily adjusted for respiratory gating only or for dual respiratory and cardiac gating (cardiac gating with blanking during inspiration), depending on the organ being imaged and the sequence used. Optical-based signal and pressure sensor based signal have been simultaneously recorded (Fig. 4b) to illustrate the effectiveness of different device to monitor cardiac and breathing movements of a given animal.

C. MR imaging

All recorded and measured parameters during CINE FLASH sequences in series 1 are reported in Table 1. Respiratory and cardiac periods were stable for each mouse during the entire examination. Mean period values ranged between 1.8 and 1.9 s for breathing and between 146 and 149 ms for heart beat. All synchronization devices enabled to perform CINE FLASH sequences and to obtain typical heart beating images series (Fig. 5).
MR images of mice heart depict low visible motion artifacts with all investigated signals used for prospective triggering as well as for retrospective ones (Fig. 6).
The mean SNR measured in the myocardium wall for all frames of the CINE FLASH acquisition is reported for each mouse in Fig. 7a and Fig. 7c for the first and second series respectively. The averaged SNR for all mice was 21.1±3.8, 20.4±4.8 and 20.1±2.6 for the optical, ECG and air pressure sensors respectively. The mean averaged SNR for all mice was 21.3±3.6, 22.3±3.8 and 21.1±3.4 for the optical, ECG and IntraGate methods respectively. No significant SNR differences were found on images acquired using the different sensors and triggering methods. On the other hand, the mean SNR measured on images acquired with the CINE FLASH sequence without synchronization (triggering option off and fixed TR adjusted to 150 ms) was significantly lower with a value of 11.7±0.5 (performed on a unique mouse). The average scan time for each sequence was slightly longer when monitoring was performed with the optical device compared to the other sensors or techniques. The latter along with the retrospective technique were similar with a fixed scan time of 399 s. However, this difference between optic and ECG was not significant to a $p \leq 0.05$ criterion. The same observation can be made with the CNR. SNR results were similar with the BB CINE FLASH with no significant difference shown between images acquired with optical gating (22.8±3.1) and ECG (22.4±5.2) gating (Fig. 8a).

Two examples of the left ventricular cavity area variation with the cardiac cycle are shown in Fig. 7b and Fig. 7d. Depending on the device or method used, the triggering point does not correspond to the same instant of the cardiac cycle, inducing a time shift between image series. The variations in delays are related to sensor location on thorax.
Finally, the synchronized MR images acquired on mice liver (data not shown) using a balanced dual cardio-respiratory triggering strategy [22] depicted no motion artifacts, even in the upper region of the liver close to the heart.

IV. DISCUSSION

With a 30 Hz bandwidth, the complex transfer function of the optical device developed was suitable for the heart beat and respiratory motion monitoring and gating. The temporal shape of the optical output signal (after filtering and amplification) however shows a considerably different pattern when compared to the characteristic pattern of the ECG. The severe low-pass filtering, allowing both a rejection of low frequency noise coming from the 50 Hz residue of the power supply and the circuit electronic noise induces low frequency oscillations. This however is not critical because the optical device has demonstrated that it is suitable for prospective gating. Nevertheless, this leaves an undeniable advantage to ECG in terms of physiological interpretation. Indeed, based on ECG-signal reading, the different heart phases can be determined. The systolic heart phase is defined as the period of ventricle contraction while the period during ventricular relaxation is defined as the diastolic heart phase. By detecting the depolarization of the ventricles on the ECG signal, the start of the systolic heart phase can be identified. Hence, an improved SNR with recent models of LED and batteries for the power supply circuit may allow a widening of the system bandwidth to keep high frequency harmonics and prevent any waveform distortions.

Full optical-based signal derived from the heart and respiratory motion was suitable for prospective triggering of heart imaging. Visible motion artifacts were comparably low on each series of mice heart MR image acquisitions triggered by the three different sensors respectively. Only artifacts caused by fast flowing blood at the end of a diastolic phase and the beginning of a systolic phase were seen on CINE FLASH images. These artifacts were anyhow suppressed afterwards using BB method (Fig. 8b). More than the image SNR, the SNR per unit of time has to be carefully considered. Results show that the different signals for prospective and retrospective synchronization techniques performed similarly. Time shift between the frames acquired with the different sensors is the major difference between the compared techniques. This time shift is different from one mouse to another. This result is hardly surprising; if for example the pressure sensor signal is correlated to heart beats, a variable delay is introduced between the heart motion and pressure signal depending on air cushion position. The same explanation may apply to the optical signal shift compared to ECG. Depending on the fiber-

optic stethoscope's depth of introduction in the esophagus, similar optical signal variations were also noticed [14]. Indeed, light reflected by tissue originates from two sources: The first one is light directly reflected from the vibrating surface induced by the proximity of the heart. The amplitude of this mechanical movement is sufficient large to induce a change in luminous flux transmitted from the illumination fiber to the receiving fiber. The other reflection source is the light backscattered by the tissue. The mean free path of absorption in tissues in the near infrared has a range of a few centimeters [24]. At this wavelength, the light easily penetrates into the tissue (diffusive media). The properties of diffusion and absorption of the medium, and thus the amount of backscattered light depends on organs in the vicinity and the layer disposition in the tissue. This disposition is continually modified by heart motion. Overall, the amount of light backscattered from the underlying volume corresponds to the signature of the cardiac motion. However the weighting of the two phenomena is unknown and deserves further study to optimize the geometry of the probe. The sequential use of two light sources of different wavelengths should help to clarify this point. Indeed, light at about 800 nm has an absorption length that is almost two orders of magnitude greater than light at about 500 nm and thus the penetration depth in tissue is significantly lower. In the latter case (green light), the effect of backscatter is minor compared to the effect of reflection at the surface.

The optical sensor and the pressure sensor perform likewise for prospective triggering and show similar variability in terms of delay between heart beats or respiratory motions and output or gating signal. However the optical sensor retains two major advantages over the pressure sensor; it is less bulky than the air cushion and the measurements are not temperature sensitive. Indeed, the small size of the optical sensor greatly facilitates its installation (more delicate with the pressure sensor), compatibility with cardiac array coils and since there is no need to press the sensor on the mouse's thorax, the latter's comfort is greatly enhanced. Moreover, the optical sensor being insensitive to temperature variations, the risk of any output signal drift due to the latter is reduced to a minimum.

The principle of the described optical fiber device is similar to the work published by Brau and co-authors [14]. However, compared to this fiber-optic stethoscope, the main differences are the ability to surface-mount the sensor rather than to insert it into the esophagus which is technically demanding. Added to this, the presented optical device (including its own interface module) was conceived such that it can directly be plugged to a commercial trigger unit with the usual adjustment parameters and it does not require any specific monitoring unit or signal processing.

Retrospective triggering method using a navigator MR signal is attractive [25]. However, some sequences such as magnetization-prepared sequences or gated hyperpolarized cardiac imaging [26] cannot be retro-gated. Moreover, this method requires magnetic gradient coils with elevated duty cycle as well as an efficient cooling circuit to prevent temperature increase due to short TR and long scan time without any pause [27]. As a matter of fact, the limited heat surface exchange in small diameter gradient coils can switch the gradient amplifiers in security mode to prevent gradient coil damage. While this approach does not require any sensor for the triggering, it is however still essential to monitor the breathing cycle and maybe more importantly the ECG in order to control the animal's vital functions [28].

During a scan, RF pulses and gradient switching induce eddy currents which disturb the ECG signal. For small flip angles, the ECG signal can be easily filtered to recover a usable signal for triggering and perform, for example, FLASH acquisitions in a CINE mode afterwards. Using SE or RARE sequence with additional FS pulse or saturation bands, ECG filtering is much more challenging. These problems are increasing with high magnetic field strength and can further result in burns on the animal due to the field concentrations on the conductive ECG leads [21, 29].

For liver imaging, when performing a multiple SE sequence, the optical sensor was used successfully for a dual cardiac and respiratory synchronization on mice. The dual triggering is particularly important to avoid artifacts in the upper part of the liver due the proximity of the heart [30].

Since light propagation in the optical fibers was free of any electromagnetic perturbation, the sensor performed well, especially when associated to a balanced acquisition over several respiratory periods [22]. These results are consistent with recent manuscripts reporting the interest of optical information measures using different apparatus, either for prospective [31] or retrospective [32] motion correction. The optical sensor may also possess a major advantage to study cardiovascular disease on animal models with heart failure. In this case, the ECG signal reflecting the pathological state is disturbed in shape and intensity leading to unreliable ECG-based triggering [33].

In conclusion, a full fiber optical-based signal derived from heart and respiratory motion was suitable for prospective triggering for heart and liver MR imaging. For cardiac MRI, the fiber optic device performed similarly to ECG. The optical fiber-based device is an attractive alternative to commercially available triggering devices for small animal MRI, especially when retrospective methods are inappropriate or in difficult environments such as high field magnets, fast gradient switching or when only a small volume is available as RF surface coils or coil arrays pressed against the chest wall.

ACKNOWLEDGMENT

The Authors thank Eduardo DaVila for assistance with CreaContour module and Audrey Pouzin for her help with optical device characterization. This work was performed within the framework of the LABEX PRIMES (ANR-11-LABX-0063) of Université de Lyon, within the program "Investissements d'Avenir" (ANR-11-IDEX-0007) operated by the French National Research Agency (ANR).

REFERENCES

[1] F. Wiesmann, M. Szimtenings, A. Frydrychowicz, R. Illinger, A. Hunecke, E. Rommel,S. Neubauer, A. Haase, "High-resolution MRI with cardiac and respiratory gating allows for accurate in vivo atherosclerotic plaque visualization in the murine aortic arch," *Magn Reson Med*, vol. 50, pp. 69-74, Jul 2003.

[2] H. R. van Genderingen, M. Sprenger, J. W. de Ridder, and A. C. van Rossum, "Carbon-fiber electrodes and leads for electrocardiography during MR imaging," *Radiology*, vol. 171, p. 872, Jun 1989.

[3] P. Choquet, C. Goetz, G. Aubertin, F. Hubele, S. Sannie, and A. Constantinesco, "Carbon tube electrodes for electrocardiography-gated cardiac multimodality imaging in mice," *J Am Assoc Lab Anim Sci*, vol. 50, pp. 61-4, Jan 2011.

[4] J. N. Amoore and J. P. Ridgway, "A system for cardiac and respiratory gating of a magnetic resonance imager," *Clin Phys Physiol Meas*, vol. 10, pp. 283-6, Aug 1989.

[5] J. P. Vallee, M. K. Ivancevic, D. Nguyen, D. R. Morel, and M. Jaconi, "Current status of cardiac MRI in small animals," *MAGMA*, vol. 17, pp. 149-56, Dec 2004.

[6] D. Abi-Abdallah, E. Chauvet, L. Bouchet-Fakri, A. Bataillard, A. Briguet, and O. Fokapu, "Reference signal extraction from corrupted ECG using wavelet decomposition for MRI sequence triggering: application to small animals," *Biomed Eng Online*, vol. 5, p. 11, 2006.

[7] K. W. Fishbein, P. McConville, and R. G. Spencer, "The lever-coil: a simple, inexpensive sensor for respiratory and cardiac motion in MRI experiments," *Magn Reson Imaging*, vol. 19, pp. 881-9, Jul 2001.

[8] N. G. Burdett, T. A. Carpenter, and L. D. Hall, "A simple device for respiratory gating for the MRI of laboratory animals," *Magn Reson Imaging*, vol. 11, pp. 897-901, 1993.

[9] S. K. Lemieux and G. H. Glover, "An infrared device for monitoring the respiration of small rodents during magnetic resonance imaging," *J Magn Reson Imaging*, vol. 6, pp. 561-4, May-Jun 1996.

[10] S. J. Wilson, I. M. Brereton, P. Hockings, W. Roffmann, and D. M. Doddrell, "Respiratory triggered imaging with an optical displacement sensor," *Magn Reson Imaging*, vol. 11, pp. 1027-32, 1993.

[11] K. P. Fichtner, V. Schirrmacher, A. Griesbach, and W. E. Hull, "In vivo 1H-NMR microimaging with respiratory triggering for monitoring adoptive immunotherapy of metastatic mouse lymphoma," *Magn Reson Med*, vol. 38, pp. 440-55, Sep 1997.

[12] J. R. Garbow, X. Lin, N. Sakata, Z. Chen, D. Koh, and G. Schonfeld, "A Simple, Robust Hardware Device for Passive or Active Respiratory Gating in MRI and MRS Experiments," *Concepts Magn Reson Part B (Magn Reson Engineering)*, vol. 21B, pp. 40-48, 2004.

[13] J. P. Legendre, R. Misner, G. V. Forester, and Y. Geoffrion, "A simple fiber optic monitor of cardiac and respiratory activity for biomedical magnetic resonance applications," *Magn Reson Med*, vol. 3, pp. 953-7, Dec 1986.

[14] A. C. Brau, C. T. Wheeler, L. W. Hedlund, and G. A. Johnson, "Fiber-optic stethoscope: a cardiac monitoring and gating system for magnetic resonance microscopy," *Magn Reson Med*, vol. 47, pp. 314-21, Feb 2002.

[15] T. Frauenrath, F. Hezel, W. Renz, G. d'Orth Tde, M. Dieringer, F. von Knobelsdorff-Brenkenhoff, M. Prothmann, J. Schultz Menger , T. Niendorf, "Acoustic cardiac triggering: a practical solution for synchronization and gating of cardiovascular magnetic resonance at 7 Tesla," *J Cardiovasc Magn Reson*, vol. 12, p. 67, 2010.

[16] T. Frauenrath, K. Fuchs, M. A. Dieringer, C. Özerdem, N. Patel, W. Renz, A. Greiser, T. Elgeti, T. Niendorf, "Detailing the use of magnetohydrodynamic effects for synchronization of MRI with the cardiac cycle: a feasibility study," *J Magn Reson Imaging*, vol. 36, pp. 364-72, Aug 2012.

[17] M. E. Crowe, A. C. Larson, Q. Zhang, J. Carr, R. D. White, D. Li, O.P. Simonetti, "Automated rectilinear self-gated cardiac cine imaging," *Magn Reson Med*, vol. 52, pp. 782-8, Oct 2004.

[18] A. C. Larson, R. D. White, G. Laub, E. R. McVeigh, D. Li, and O. P. Simonetti, "Self-gated cardiac cine MRI," *Magn Reson Med*, vol. 51, pp. 93-102, Jan 2004.

[19] A. C. Brau and J. H. Brittain, "Generalized self-navigated motion detection technique: Preliminary investigation in abdominal imaging," *Magn Reson Med*, vol. 55, pp. 263-70, Feb 2006.

[20] R. S. Khandpur, Ed., *Handbook of Biomedical Instrumentation*. Tata McGraw-Hill Professional, 2003, p.^pp. Pages.

[21] H. Kugel, C. Bremer, M. Puschel, R. Fischbach, H. Lenzen, B. Tombach, H. Van Haken, W. Heindel, "Hazardous situation in the MR bore: induction in ECG leads causes fire," *Eur Radiol*, vol. 13, pp. 690-4, Apr 2003.

[22] L. M. Baboi, L. Milot, C. Lartizien, C. Roche, J. Y. Scoazec, F. Pilleul, O. Beuf, "Synchronization strategies in T2-weighted MR imaging for detection of liver lesions: Application on a nude mouse model," *Biomed Imaging Interv J*, vol. 3, pp. 1-9, 2007.

[23] O. Beuf, C. Lartizien, L. Milot, L. Baboi, C. Roche, J. B. Langlois, J. Y. Scoarzec, F. Pilleul, "Multimodal imaging for the detection and characterization of liver lesions in a mouse model of neuroendocrine tumor," *Gastroenterol Clin Biol*, vol. 32, pp. 32-40, Jan 2008.

[24] J. Falconet, R. Sablong, E. Perrin, F. Jaillon, and H. Saint-Jalmes, "Analysis of simulated and experimental backscattered images of turbid media in linearly polarized light: estimation of the anisotropy factor," *Appl Opt*, vol. 47, pp. 5811-20, Nov 1 2008.

[25] E. Heijman, W. de Graaf, P. Niessen, A. Nauerth, G. van Eys, L. de Graaf, K. Nicolay, G. J. Strijkers, "Comparison between prospective and retrospective triggering for mouse cardiac MRI," *NMR Biomed*, vol. 20, pp. 439-47, Jun 2007.

[26] A. Z. Lau, A. P. Chen, N. R. Ghugre, V. Ramanan, W. W. Lam, K.A. Connelly, G.A. Wright, , "Rapid multislice imaging of hyperpolarized 13C pyruvate and bicarbonate in the heart," *Magn Reson Med*, vol. 64, pp. 1323-31, Nov 2010.

[27] S. Miraux, G. Calmettes, P. Massot, W. Lefrancois, E. Parzy, B. Muller, L. M. Arsac, V. Deschodt-Arsac, J. M. Franconi, P. Diolez, E. Thiaudière, "4D retrospective black blood trueFISP imaging of mouse heart," *Magn Reson Med*, vol. 62, pp. 1099-105, Nov 2009.

[28] B. F. Coolen, T. Geelen, L. E. Paulis, A. Nauerth, K. Nicolay, and G. J. Strijkers, "Three-dimensional T(1) mapping of the mouse heart using variable flip angle steady-state MR imaging," *NMR Biomed*, vol. 24, pp. 154-62, Oct 19 2011.

[29] V. Detti, D. Grenier, E. Perrin, and O. Beuf, "Assessment of radiofrequency self-heating around a metallic wire with MR T1-based thermometry," *Magn Reson Med*, vol. 66, pp. 448-55, Feb 2011.

[30] L. Baboi, F. Pilleul, L. Milot, C. Lartizien, G. Poncet, C. Roche, J. Y. Scoarzec, O. Beuf, "Magnetic resonance imaging follow-up of liver growth of neuroendocrine tumors in an experimental mouse model," *Magn Reson Imaging*, vol. 28, pp. 264-72, Feb 2010.

[31] B. C. Andrews-Shigaki, B. S. Armstrong, M. Zaitsev, and T. Ernst, "Prospective motion correction for magnetic resonance spectroscopy using single camera retro-grate reflector optical tracking," *J Magn Reson Imaging*, vol. 33, pp. 498-504, Feb 2011.
[32] M. Korn, R. Umathum, J. Schulz, W. Semmler, and M. Bock, "Optically detunable, inductively coupled coil for self-gating in small animal magnetic resonance imaging," *Magn Reson Med*, vol. 65, pp. 882-8, Mar 2011.
[33] F. Kober, I. Iltis, P. J. Cozzone, and M. Bernard, "Cine-MRI assessment of cardiac function in mice anesthetized with ketamine/xylazine and isoflurane," *Magma*, vol. 17, pp. 157-61, Dec 2004.

FIGURES

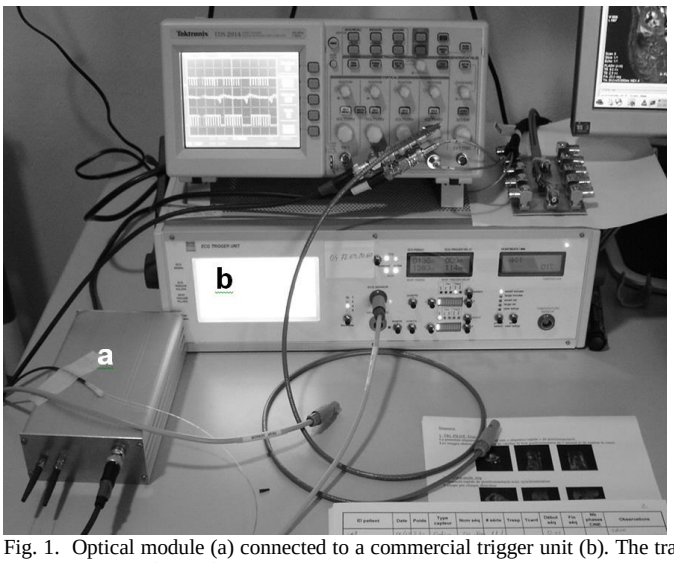

Fig. 1. Optical module (a) connected to a commercial trigger unit (b). The transmitter and receiver fibres and the electrical output coaxial cable are seen in front of the optical module.

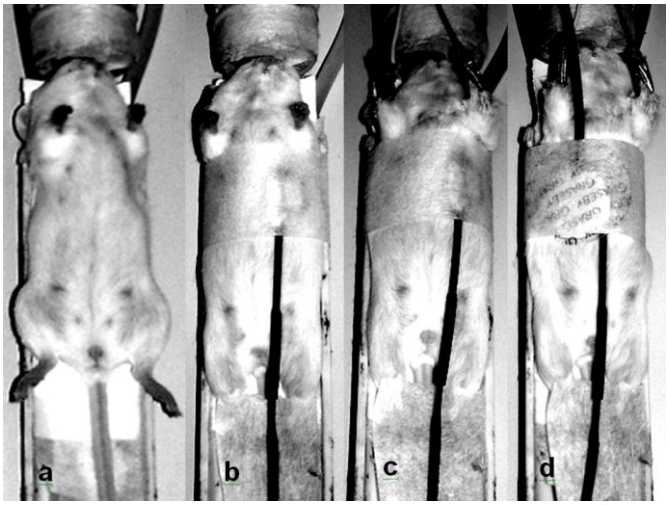

Fig. 2. Sensor mounting procedure on the anesthetized mouse: (a) before and (b) after optical fiber pair fixation on thorax, (c) electrodes placements on the front legs and (d) air cushion.

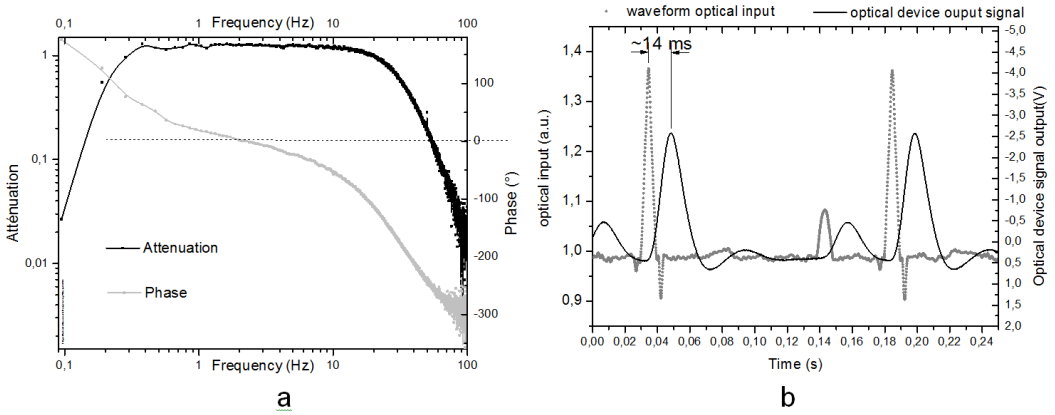

Fig. 3. (a) Bode diagram of the optical device. The band pass filter characteristics fit the expected attenuation specifications. (b) Optical device response to a typical ECG waveform excitation signal. At about 14 ms peak delay, a curve broadening can be noticed.

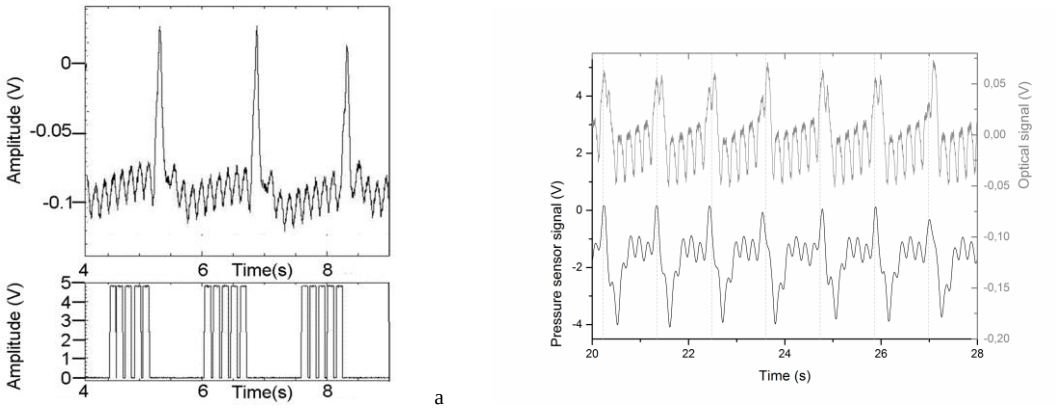

a b

Fig. 4. (a) The optical-based input signal (top) shows large peaks attributed to respiratory cycle and small oscillations to heart motion. The derived gating signal (bottom) from trigger unit outputs is used to synchronize MRI acquisitions. (b) Simultaneous acquisition of optical-based signal (top) and pressure sensor signal (bottom) to monitor respiration and heart motions.

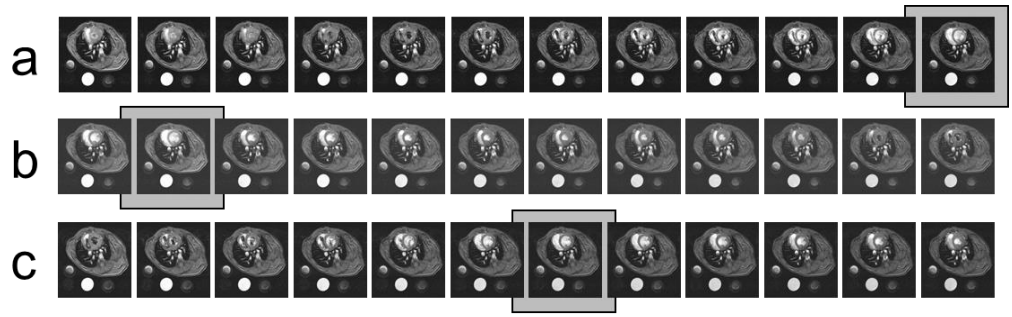

Fig. 5. Example of MRI series acquired with the CINE sequence using (a) optical device, (b) ECG and (c) air cushion.

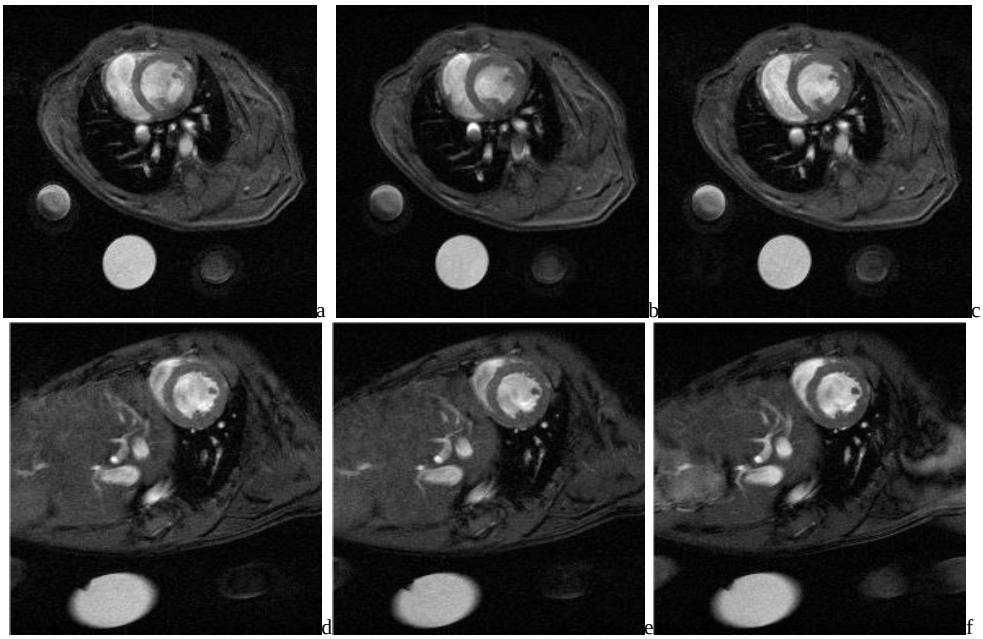

a b c

d e f

Fig. 6. MRI images acquired on a first mouse using a CINE FLASH sequence corresponding approximately to the same cardiac phase with: (a) optical device, (b) ECG and (c) air cushion. The images displayed do not correspond necessarily to the same frame in the CINE sequence. MRI images acquired on a second mouse using a CINE FLASH sequence corresponding approximately to the same cardiac phase with: (d) optical device, (e) ECG and (f) IntraGate.

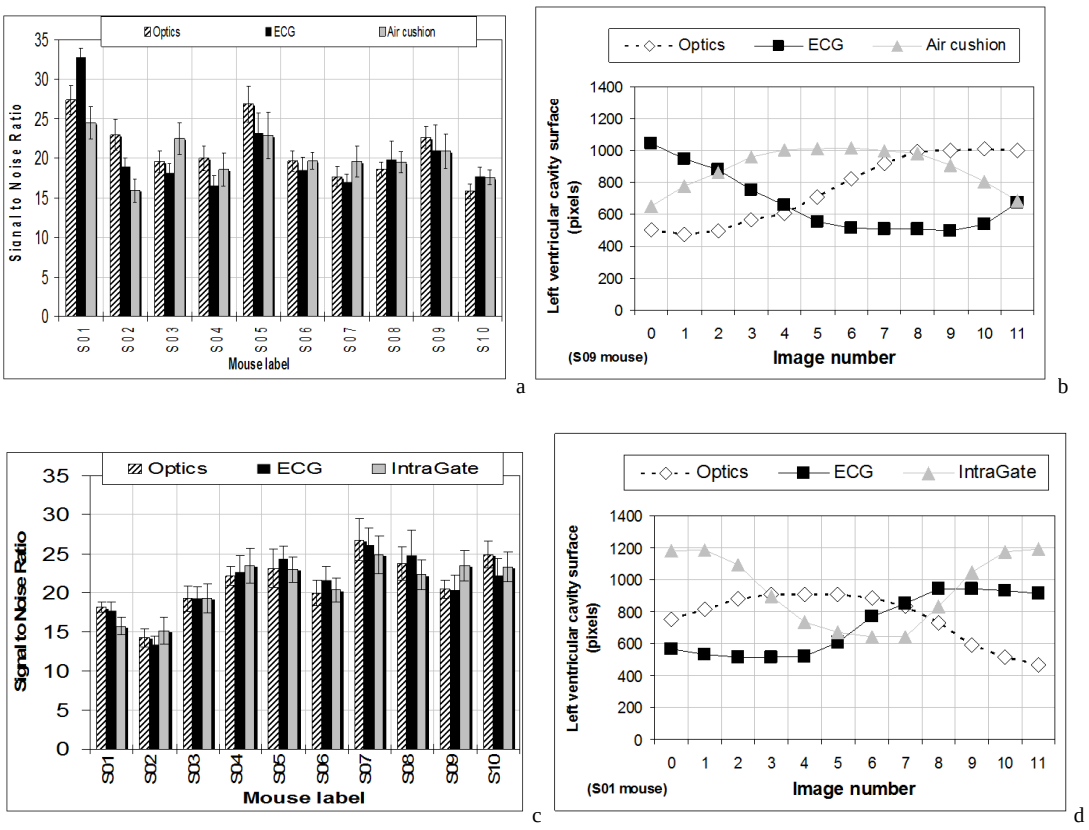

Fig. 7. (a) Mean SNR-values measured on myocardium wall for the three different sensors and for each mouse. (b) Example of evolution of the left ventricular cavity surface with frame number and corresponding to different phases of the cardiac cycle, depending on sensor used. (c) Mean SNR-values measured on myocardium wall for the three different methods and for each mouse. (d) Example of evolution of the left ventricular cavity surface with frame number and corresponding to different phases of the cardiac cycle, depending on method used.

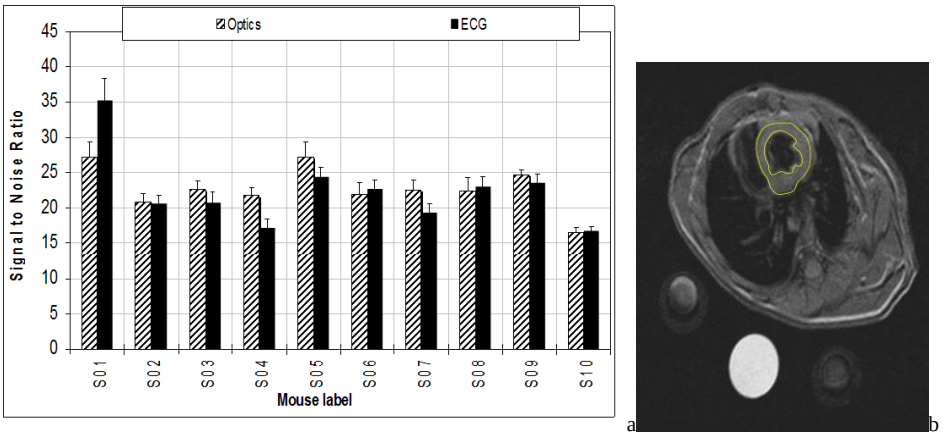

Fig. 8. Black Blood CINE FLASH Sequence. (a) Mean SNR-values measured on myocardium wall with two different methods and for each mouse. Mean SNR-values were 22.8 ± 3.1 and 22.4 ± 5.2 for optics and ECG respectively. (b) Example of MR image acquired with ECG sensor. The ROI matching to the myocardium wall is overlaid on the images.

TABLE I

MEAN ± STANDARD DEVIATION VALUES OF PARAMETERS MEASURED DURING ACQUISITION AND ON CINE FLASH IMAGES OF SERIES 1

	Respiratory period (s)	Cardiac period (ms)	Scan time (s)	SNR	CNR
Optical	1.8±0.2	149±14	432±90	21.1 ± 3.8	20.8 ± 2.1
ECG	1.8±0.2	147±16	384±102	20.4 ± 4.8	22.3 ± 2.8
Pressure	1.9±0.2	146±13	414±78	20.1 ± 2.6	22.8 ± 3.1